Intention Prediction and Mixed Strategy Nash Equilibrium-Based Decision-Making Framework for Autonomous Driving in Uncontrolled Intersection

Jiangfeng Nan, Weiwen Deng, *Member, IEEE*, and Bowen Zheng

***Abstract*—Decision-making in uncontrolled intersection is one of the main challenges in urban autonomous driving. This paper proposed a new decision-making framework in uncontrolled intersection based on the intention prediction method and Mixed Strategy Nash Equilibrium theory. The framework is a three-stage method: target vehicle motion prediction, driving mode decision, and motion planning. The driving intention (left turn, right turn, or go straight) of the target vehicle at the intersection can be predicted using the combination algorithm of GMM-HMM and SVM. According to the driving intention and road structure, the trajectory fitting module would use the Bezier curve to fit the predicted trajectory of a target vehicle. Furthermore, combined with trajectories of the ego vehicle, the S-T diagram is used to judge whether there is a spatio-temporal conflict point of the target vehicle and ego vehicle. If there is a conflict point of the target vehicle and ego vehicle, the driving mode ('yield' or 'cross') of the ego vehicle is selected by using the Mixed Strategy Nash Equilibrium theory. This method can not only avoid premature or unnecessary deceleration due to conservation but also avoid a collision or violent deceleration due to greed. According to the driving mode, the planning module uses the model predictive control algorithm to determine the optimal acceleration strategy. Have been verified by the vehicle test, it indicates that the proposed decision-making framework can make ego vehicles pass through the intersection safely and comfortably.**

***Index Terms*—Autonomous driving, mixed strategy nash equilibrium theory, model predictive control and intention prediction.**

I. Introduction

AUTONOMOUS driving will become an effective means to solve existing traffic problems such as traffic congestion, vehicle pollution and traffic accidents. In order to massively deploy autonomous vehicles in urban areas, autonomous vehicles must be able to pass through the intersection safely, comfortably and efficiently [1]. According to statistics, 40% of traffic accidents in Europe occur in intersection scenes [2]–[4], of which 96% are caused by improper operation by drivers [5]. Another statistics shows that 21.5% of fatalities and even 40% of all accidents in the US happening at intersections [6]. Common sense is that taking a conservative driving strategy can avoid accidents. However, driving too conservatively is not only inefficient, but also easily leads to accidents and deadlocks [7]. Strategy of Waymo, a Google company, in the intersection is very conservative (always stop briefly when passing the intersection), but there still have been accidents [8].

The uncertainty of motion of traffic participants and the indescribability of interaction of vehicles are the key challenges of autonomous vehicles' decision at intersections. In order to solve this problem, a three-stage method solving framework is presented: target vehicle motion prediction, multi-vehicle interaction and motion planning. Target vehicle motion prediction can be solved in two ways: direct prediction and indirect prediction. The prediction based on physical model is a classic kind of direct prediction, which only has high accuracy in predicting the trajectory of the next 1 second [9]–[11], which obviously cannot meet the prediction time required for decision-making in intersection. In recent years, LSTM [12] has also become a common direct prediction method, but its maximum prediction time has only extend to 2 seconds, with tradeoff of greater amount of calculation for practical application. Lei Lin *et al.* [13] proposed a vehicle trajectory prediction method using LSTMs with spatial-temporal attention mechanisms (STA-LSTM), in which the historical trajectories on the target vehicle and neighboring vehicles have been taken into account. The motion prediction method based on intention prediction is an indirect trajectory prediction method, which can predict the future trajectory for a longer time by first predicting the driver's driving intention and then fitting the future trajectory. At present, driving intention prediction mainly uses machine learning algorithm. Compared with the method using classifier, the inference result of intention prediction method [14] through IMM is more continuous. In [15], dynamic Bayesian network, HMM and SVM are compared. It is considered that the prediction effect of dynamic Bayesian network and SVM is better than HMM method, and the prediction accuracy can reach 90%, 1.6 second before the vehicle reaches the intersection. To improve the accuracy of trajectory prediction, Ting Zhang *et al.* [16] proposed a vehicle motion prediction method at intersections based on the turning intention and prior trajectories model. In structured roads, indirect prediction methods based on intention prediction usually

Manuscript received 11 February 2022; revised 30 May 2022; accepted 24 June 2022. Date of publication 29 June 2022; date of current version 17 October 2022. This work was supported in part by the National Key R&D Program of China under Grant 2018YFB0105103 and in part by the National Natural Science Foundation of China under Grant U1864201. The review of this article was coordinated by Dr. Marilisa Botte. *(Corresponding author: Weiwen Deng.)*

Jiangfeng Nan and Bowen Zheng are with the School of Transportation Science and Engineering, Beihang University, Beijing 100191, China (e-mail: nanjiangfeng@buaa.edu.cn; zbw94@buaa.edu.cn).

Weiwen Deng is with the School of Transportation Science and Engineering, Beihang University, Beijing 100191, China, and also with the Beijing Advanced Innovation Center for Big Data and Brain Computing, Beihang University, Beijing 100191, China (e-mail: wdeng@buaa.edu.cn).

Digital Object Identifier 10.1109/TVT.2022.3186976

achieve better results than direct prediction methods. This is attributed to the transformation from the high-dimensional motion prediction problem to the low-dimensional intention prediction based on the road structured information. Then the calculated result of intention prediction can guide the motion prediction, achieving a longer horizon of the predicted trajectory. However, the effect of this method is strongly influenced by the results of intention prediction. Therefore, it is urgent to improve the accuracy of intention prediction.

The interaction with surrounding vehicles is a key task of intersection decision-making. Andrei *et al.* [17] used the rule-based method to solve the challenge of complex interaction with surrounding vehicles. Although this method is easy to implement, it fails to deal with scenes outside the preset rules, rendering a poor generalization performance. Li G *et al.* [18] used a Deep Deterministic Policy Gradient network (DDPG) to tackle the challenge of complex interaction with surrounding vehicles at the intersection. In this paper, the speed of the ego vehicle and the relative distances with the surrounding vehicle have been taken as the inputs of the model, while the throttle is the output. Experimental results have shown that this method can make the ego vehicle pass the intersection safely, efficiently, and comfortably. However, it only takes effect when the ego vehicle goes straight. In [19], multi-vehicle interaction behavior is modeled as an incomplete information static game to improve the accuracy of vehicle intention prediction. In [20], a game model of human-vehicle interaction is established, by which the probabilities of six human-vehicle interaction scenarios (people give way to cars, cars give way to people, etc.) are obtained. In [21], a Road Side Controller collects the status information of surrounding vehicles using V2X technology, and uses game theory to command vehicles to pass through the intersection. Cheng C *et al.* used repeated game theory to avoid collisions caused by multi-vehicle interaction at intersections, which redefines a payoff function composed of safety, speed and control indicators, and uses Pareto optimality to obtain the strategy of maximizing the payoff of the game [22]. Rahmati *et al.* [23] proposed an intersection decision-making method using game theory, which needs to calibrate a large number of parameters. In general, rule-based interaction methods heavily rely on the preset rules, leading to a poor generalization performance. Meanwhile, the interactivity method based on reinforcement learning is difficult to prove its security due to its poor interpretability. Compared with these two methods, the game theory-based method has both interpretability and generalization. However, the uncertainty of the interaction process is not fully considered in the existing game theory-based methods.

In recent years, many methods have been used for intersection motion planning. Most of these methods provides the suggest speed or acceleration to autonomous vehicles. The optimal acceleration on the desired path can be determined by using the partially observable Markov decision process [24]–[26]. In [27], DQN is used as a longitudinal motion planner, including three different strategies: "time-to-go", "sequential actions" and "creep-and-go" to determine whether the agent accelerates, decelerates or maintains the original speed. In [14] and [28], taking the first-order inertial element as the vehicle acceleration response model, the acceleration is planned by using the Model Predictive Control (MPC). Johannes *et al.* [29] used MPC algorithm to plan the longitudinal jerk. By contrast, the MPC-based motion planning method has more security and stability. However, making reasonable states reference and loss function is the biggest challenge of MPC-based motion planning.

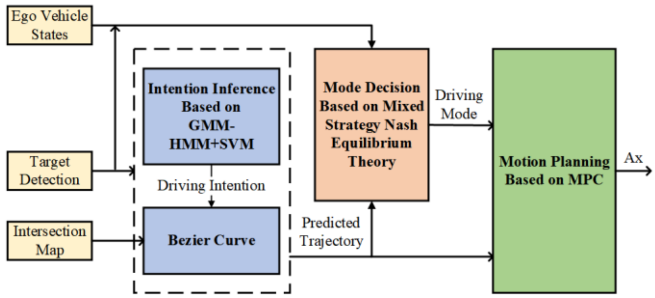

Fig. 1. Framework of decision-making.

In the study of decision-making for autonomous driving in intersection, most works often focus on a single problem, ignore other parts and the relationship between them, and fail to put forward a complete decision-making framework. For example, although Jeong Y *et al.* [14] focus on trajectory prediction and motion planning, forget to considered the interaction between vehicles. Cheng C *et al.* [22] only pay attention to the interaction between vehicles at intersections independently, but ignore trajectory prediction and motion planning.

This paper provides a strategy for the decision-making for autonomous driving in intersections, including three parts: target vehicle motion prediction, multi-vehicle interaction and motion planning, and presents a new decision-making framework in uncontrolled intersection, as shown in Fig. 1. Firstly, the intention prediction module predicts driver's driving intention using target vehicle state information. The trajectory fitting module fits future trajectory of the target vehicle according to the intention prediction results and the intersection map. Then, the driving mode decision module selects the target driving mode using the Mixed Strategy Nash Equilibrium theory according to the state of the target vehicle and ego vehicle. Finally, the motion planning module uses MPC to obtain the desired acceleration. Main contributions of this paper are: (1) a complete new decision-making framework in uncontrolled intersection is proposed. (2) In order to improve the accuracy of intention prediction, an intention prediction method combining GMM-HMM and SVM is proposed. (3) The Mixed Strategy Nash Equilibrium theory is applied to driving mode decision-making ('yield' or 'cross'), which not only avoids premature or unnecessary deceleration due to conservation, but also avoids collision or violent deceleration due to greed. (4) Through the S-T diagram, a reasonable reference state is provided for MPC, which makes the control effect more comfortable while meeting the safety constraints.

The rest of the paper is organized as follows. In Section II, this paper will introduce the driving intention prediction algorithm. The driving mode decision-making method based on Mixed Strategy Nash Equilibrium theory is presented in Section III. In Section IV, the motion planning based on MPC is introduced.

In Section V, in order to verify the effectiveness of the decision-making framework, a vehicle test is performed and the paper is finally concluded in Section VI.

II. Driving Intention Prediction and Trajectory Fitting of Target Vehicle

Human can be regarded as a device composed of a large number of intentions, and each intention has its own specific control method and internal state [30]. In the intersection, the driving intention can be divided into "straight", "left turn" and "right turn". Because it is impossible to determine how many states each driving intention has and the specific definition of each state, this paper uses hidden Markov model (HMM) to model this process. However, classic HMM uses discrete variables as observations. Since the observations of the state are a set of continuous variables, the Gaussian Mixture Model (GMM) is used to describe the emission probability of these observations. This hidden Markov model is called Gaussian mixture model -hidden Markov model (GMM-HMM).

A. GMM-HMM and SVM-Based Driving Intention Prediction

HMM is a special form of Markov model, and also obeys the basic properties of Markov process, that is, future states depend only on the current state, not on the events that occurred before it. The model parameters of HMM include initial probability, state transition probability and emission probability. The traditional HMM is only available for the situation of discrete observations, where a matrix could be used to describe its emission probability. As the observations in this paper are continuous, a matrix cannot handle this situation. Therefore, this paper uses GMM to fit the emission probability in HMM. The parameter set of GMM-HMM is $\boldsymbol{\lambda} = \{\pi, \mathbf{A}, \mathbf{C}, \mu, \boldsymbol{\Sigma}\}$, will be describe down below.

The initial probability matrix π is defined as

$$\pi = [\pi_i],\ 1 \le i \le N, \tag{1}$$

where π_i is the probability that the state at the initial time is state i.

The state transition probability matrix A of HMM is defined as

$$A = [a_{ij}],\ a_{ij} = P\left(q_{t+1}^j \left| q_t^i \right.\right),\ 1 \le i, j \le N, \tag{2}$$

where a_{ij} is the probability of transition from state i to state j. $N$is the number of hidden states of HMM. q_t^i indicates that the hidden state at time t is i.$\mathbf{C}$, $\boldsymbol{\mu}$ and $\boldsymbol{\Sigma}$ are parameters of GMM, which is used to describe the emission probability at state i:

$$b_i(\mathbf{O}) = \sum_{m=1}^{M} C_{im} N(\mathbf{O} \left| \boldsymbol{\mu}_{im}, \boldsymbol{\Sigma}_{im} \right.), \tag{3}$$

where $\mathbf{O}$ is the observations. Emission probability $b_i(\mathbf{O})$ means the probability of obtaining observations $\mathbf{O}$ at state i.C_{im} is the mixing coefficient of the m-th Gaussian model. M is the number of Gaussian models. $\boldsymbol{\mu}_{im}$ is the means of the m-th Gaussian model. $\boldsymbol{\Sigma}_{im}$ is the covariance of the m-th Gaussian model.

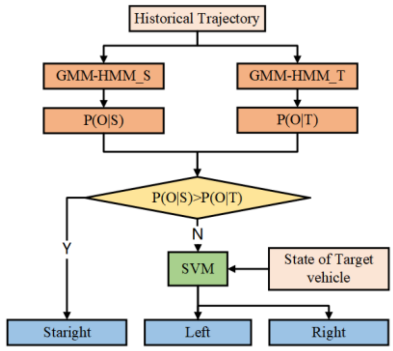

Fig. 2. Driving intention prediction.

Considering the model accuracy and complexity, the number of Gaussian models is set to 2.

Support Vector Machine (SVM) is a typical algorithm for solving classification problems, which achieves the purpose of classification by constructing hyperplane in feature space [31]. The hyperplane in the feature space can be described as

$$\boldsymbol{\omega}^T \mathbf{x} + b = 0. \tag{4}$$

The distance from the sample point $\mathbf{x}_n$ to the hyperplane is

$$r_n = \frac{\left| \boldsymbol{\omega}^T \mathbf{x}_n + b \right|}{\|\boldsymbol{\omega}\|}. \tag{5}$$

The goal of training SVM is to find the hyperplane with "maximum margin" for nearest separate class points. Therefore, the model parameters$\boldsymbol{\omega}$ and b can be described as

$$\boldsymbol{\omega}, b = \arg\max_{\boldsymbol{\omega}, b} \{\min[r_n]\}, n = 1, 2, \cdots N, \tag{6}$$

where $N$is number of samples.

Firstly, the GMM-HMM model was used to judge whether the driving intention of the target vehicle is 'straight' or 'turn'. If the driving intention is judged as the 'turn', the SVM model is adopted to distinguish whether it is 'turn left' or 'turn right'. The input of the SVM model is the features of the target vehicle at the current moment, and the output is the driving intention of the target vehicle ('turn left' or 'turn right'). The selection method of target vehicle features will be described in the next section.

Two separate GMM-HMM model of "straight" and "turn" driving intention are established respectively. Intention prediction of the target vehicle can be regarded as the probability calculation problem of the HMM, that is, the probability of the observation is calculated when the HMM is known. The historical trajectory data (observation) of the target vehicle is obtained through the onboard sensor, and the forward algorithm is used to calculate the probability of the observation in the case of "straight" model and " turn " model respectively. Then, the one with greater probability will be picked as result. If the predicted driving intention is "turn", SVM further judges whether the driving intention is "turn left" or "turn right" according to the state of the target vehicle. The process of intention prediction is shown in Fig. 2.

In Fig. 2, GMM-HMM-S is the model of "straight" driving intention while GMM-HMM-T is for "turn" driving intention.

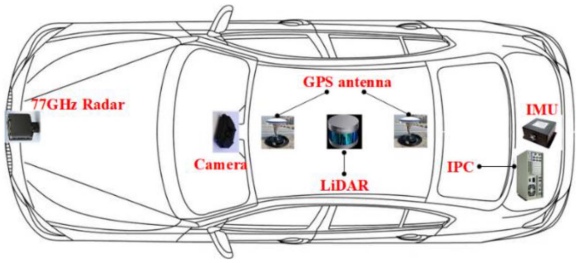

Fig. 3. The data-collection vehicle.

P(O|S) is the probability of the observations calculated in the case of "straight" model while P(O|T) is for "turn" model.

B. Data Acquisition and Feature Selection

In order to train models and acquisition vehicle to collect the driving data in intersection. The data-collection vehicle is equipped with sensors such as GPS, front camera, IMU, lidar, radar and industrial computer (IPC) for recording driving data, as shown in Fig. 3.

To train the model, more than 220000 samples were collected, including driving data under "straight", "left turn" and "right turn" conditions. Five different drivers were selected as participants in the experiment to collect driving data. They drove the data-collection vehicle to perform operations of "go straight", "turn left" and "turn right" repeatedly in the same intersection, while the data-collection vehicle recorded their driving data. The raw data were collected at 100 Hz, including latitude, longitude, heading angle, vehicle speed, yaw rate, longitudinal acceleration, lateral velocity, lateral acceleration, and timestamps. Meanwhile, each data sample was labeled with an experimental number and condition ("go straight", "turn left" or "turn right"). After processed, the features of collected driving data include the distance S from the intersection (when vehicles reach the intersection, $S = 0$), lateral offset (based on the lane centerline), heading angle (the lane direction is 0 degrees and the left is positive), yaw rate, vehicle speed, longitudinal acceleration, lateral speed and lateral acceleration. In this paper, the correlation analysis method is used to select features, which improves the accuracy of the model and reduces the complexity of the model by merge the observations with high correlation.

The mean of a driving feature i is defined as

$$\bar{x}_i(S) = \frac{1}{n}\sum_{j=1}^{n} x_{ij}(S), \tag{7}$$

where x_{ij} is the value of feature i at the j-th sample. n is the number of samples. The mean of a driving feature represents the "average" performance of most drivers in intersection.

The mean of driving features are shown in Fig. 4. "S", "L" and "R" stands for moving "straight", "left" and "right". It can be seen from the figure that lateral acceleration (Fig. 4.a), yaw rate (Fig. 4.d) and lateral velocity (Fig. 4.f) have high correlation in all conditions. Calculated coefficients verified this hypothesis, as shown in Table I below.

As can be seen from Table I, there is a very high correlation among yaw angular velocity (AVZ), lateral velocity (VY) and lateral acceleration (AY). Therefore, only the yaw rate is selected as the feature in the three observations. Finally, the distance from the intersection, lateral offset, heading angle, yaw rate, vehicle speed and longitudinal acceleration are regard as features.

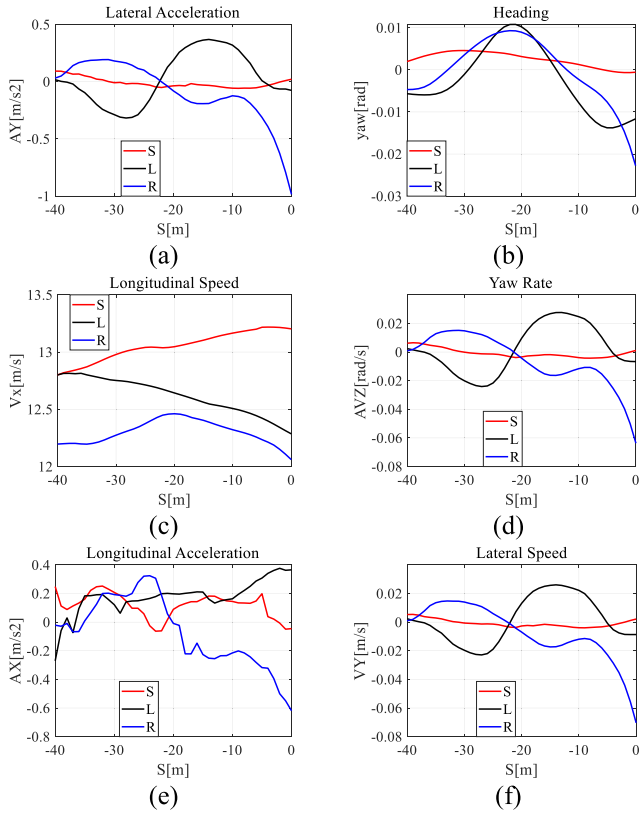

Fig. 4. Features of driving data.

TABLE I
CORRELATION COEFFICIENTS

	$r(AVZ,VY)$	$r(AVZ,AY)$	$r(VY,AY)$
"straight"	0.9806	0.9875	0.9914
"turn left"	0.9886	0.9833	0.9940
"turn right"	0.9980	0.9926	0.9971

C. Model Training and Validation

Driving intention prediction needs to be completed before the vehicle enters the intersection. In this paper, the scenario for intention prediction is called the pre-intersection scenario, which is defined as

$$\varepsilon = \{\mathbf{X}(S)\,|-40 \le \mathrm{S} \le 0\,\}, \tag{8}$$

where $\mathbf{X}$ is the vector of features of the driving data.

According to the feature selection results, the vector of features of GMM-HMM at time t is

$$\mathbf{O}_t = [S(t), L(t), yaw(t), Vx(t), AVZ(t), AX(t)], \tag{9}$$

where $S(t)$, $L(t)$, $yaw(t)$,$V_x(t)$, $AVZ(t)$ and $AX(t)$ are the distance from the intersection, lateral offset, heading angle,

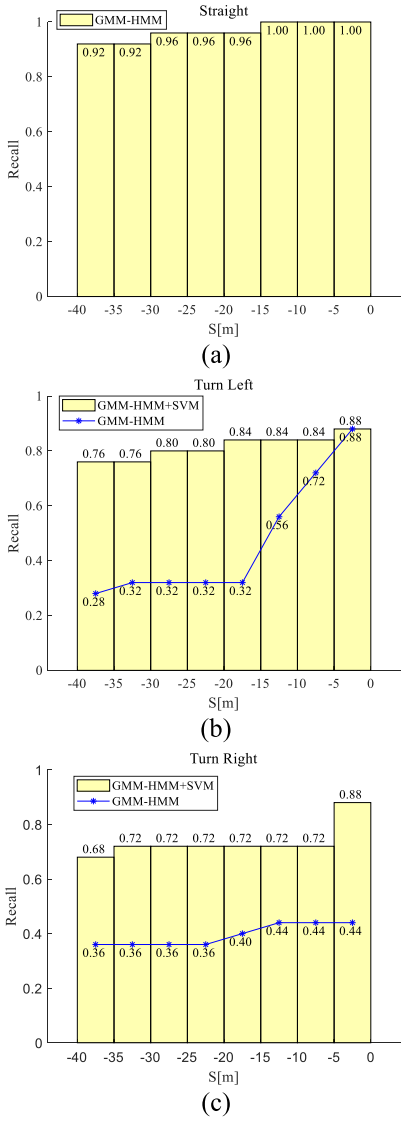

Fig. 5. Accuracy of intention prediction algorithm.

yaw rate, vehicle speed and longitudinal acceleration at time t respectively.

In the pre-intersection scenario, the time series of feature vector is described as $\mathbf{O} = (\mathbf{O}_1, \mathbf{O}_2, \cdots, \mathbf{O}_T)$. According to the principle of maximum likelihood estimation [32], training model $\boldsymbol{\lambda}$ is the process of finding a set of model parameters, which can maximize the probability $P(\mathbf{O}|\boldsymbol{\lambda})$ of the time series of feature vectors being sampled. The training data are divided into "straight" and "turn". Using two sets of data, "straight" GMM-HMM (GMM-HMM-S) and "turning" GMM-HMM (GMM-HMM-T) are trained by EM algorithm [33].

Label the turning data as "left turn" or "right turn", and use the sequential minimum optimization algorithm (SMO) [34] to train the SVM model.

In order to verify the accuracy of the algorithm, the algorithm is tested, and the test results are shown in the Fig. 5.

Fig. 5 shows that the prediction accuracy of GMM-HMM is very high when predicting "straight", and can achieve more than 92% when 40 meters away from the intersection. However, if

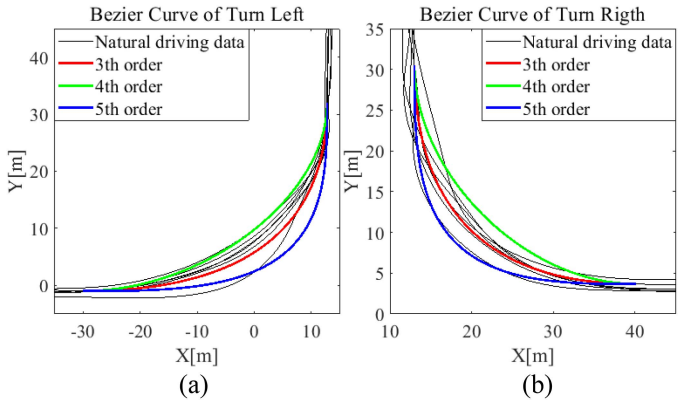

Fig. 6. Bezier curve of turn.

GMM-HMM is used to distinguish whether the driving intention is "left turn" or "right turn", the prediction accuracy is unsatisfactory. GMM-HMM always mistakenly identifies "left turn" as "right turn", or "right turn" as "left turn", rather than mistakenly identifying them as "straight", which shows that GMM-HMM can accurately identify "straight" and "turn" (including left and right). Therefore, after "straight" and "turn" are classified by GMM-HMM, SVM is used to subdivide "left turn" and "right turn" in the "turn" intention. The results show that prediction accuracy for "left turn" intention and "right turn" intention is significantly improved after using SVM to reclassify driving intention.

D. Bezier Curve-Based Trajectory Fitting Algorithm

After predicting the driving intention of the target vehicle, the Bessel curve is used to fit the future trajectory of the target vehicle. Bezier curve of order n is defined as

$$P(t) = \sum_{i=0}^{n} P_i C_n^i t^i (1-t)^{n-i}, t \in [0,1], \tag{10}$$

where P_i is the control point. C_n^i is the binomial coefficients. $t$is the parameter that predicts waypoints.

Fig. 6 shows that the third-order Bezier curve is more consistent with the natural driving data.

III. Mixed Strategy Nash Equilibrium Theory-Based Driving Mode Decision Method

When there is a conflict point of target vehicle and ego vehicle, the ego vehicle faces a driving mode decision-making problem: yield or cross. This is a multi-objective decision-making problem that needs to comprehensively consider collision risk, efficiency and comfort. The driving mode ("yield" or "cross") of the ego vehicle is selected by using the Mixed Strategy Nash Equilibrium theory in this paper.

A. Game Definition

As shown in Fig. 7, when the target vehicle turns left, there is a possible conflict point between the ego vehicle and the target vehicle. To get through the intersection safely, both target

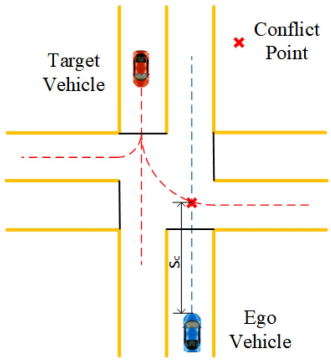

Fig. 7. Description of conflict of target vehicle and ego vehicle.

vehicle and ego vehicle need to make a decision: yield or cross. This process can be modeled as a game in which both vehicles are two players in the game. This game can be seen as a non-cooperative game process, in which each player tries to maximize their reward in the game. The reward rules for each player are the same, considering security, efficiency and comfort. Each player makes decisions according to the instantaneous state of the current moment and the prediction of the future, so as to maximize the reward. The game is defined as

$$G = (N, A, U), \tag{11}$$

where N is a set of all game participants.$A$is the action set of game participants. $U$is the revenue set of game participants. In this game, the player set is $N = (T\arg etVehicle, EgoVehicle)$. The set of actions that each player can take is $A = (Yield, Cross)$.

In the game, when no player can improve his income by changing his strategy alone, the Nash equilibrium is reached. The mathematical definition of Nash equilibrium [27] is

$$U_i\left(s_i^*, s_{-i}^*\right) \geq U_i\left(s_i, s_{-i}^*\right), i \in N, \tag{12}$$

where $U_i$is the payoff function of player i. $s_i$is the action performed by player i. $s_{-i}$is the set of actions performed by players other than player i. $s_i^*$is the action performed by player $i$when reaching Nash equilibrium.

B. Payoff Functions Formulation

In this game, the factors considered by the players are safety, efficiency and comfort. The payoff function is the mathematical form of the considered factors. Safety is regards as a constraint, that is, collision must be avoided in any case. In the intersection scenario, we can only avoid deceleration to ensure that the efficiency is not reduced, and cannot improve the efficiency by accelerating. If the efficiency can be improved by accelerating, the result of speed optimization will be to continuously increase the speed, which obviously does not meet the requirements.

For ego vehicle, there are four game results. The best is that the ego vehicle crosses and the target vehicle yields. The second best result is that the ego vehicle yields and the target vehicle crosses. At this time, the ego vehicle can brake with the most comfortable deceleration that can avoid collision. The two undesirable results are that the ego vehicle and the target vehicle choose to yield or cross at the same time. When both the ego vehicle and the target vehicle cross, the collision risk will be increased. When both the ego vehicle and the target vehicle yield, it will lead to unnecessary loss of efficiency.

TABLE II
PAYOFF MATRIX

Players	Target Vehicle		
Ego Vehicle	Actions	Yield	Cross
	Yield	a_4	a_2
	Cross	a_1	a_3

In order to avoid the influence caused by different dimensions, the acceleration is regards as the payoff function of each case. Four possible scenarios should be considered. In "ego vehicle crosses and the target vehicle yield" scenario, the ego vehicle can safely pass through the intersection without changing the speed, so the expected acceleration of the ego vehicle is

$$a_1 = 0. \tag{13}$$

In case of ego vehicle yields and the target vehicle crosses, the ego vehicle can slow down "calmly" to avoid collision. The expected acceleration of the main vehicle is

$$a_2 = \frac{2\left(S_E - D_{safe} - v_E t_T\right)}{t_T^2}, \tag{14}$$

where S_E is the distance from the ego vehicle to the conflict point. D_{safe} is the minimum safe distance. v_E is the speed of the ego vehicle. t_T is the time when the target vehicle reaches the conflict point.

When both the ego vehicle and the target vehicle refuse to yield, the ego vehicle can only brake in the next decision-making cycle of driving mode as soon as possible. At that time, the expected acceleration of the ego vehicle is

$$a_3 = \frac{2(S_E - D_{safe} - v_E t_T)}{\left(t_T - \Delta t\right)^2}, t_T > \Delta t, \tag{15}$$

where Δt is the period of decision-making of driving mode.

When both the ego vehicle and the target vehicle yield, although the ego vehicle can slow down "calmly" to avoid collision, it will reduce efficiency. In general, traffic time can be used to quantify efficiency. In order to avoid the influence of different dimensions, equivalent acceleration is used to quantify efficiency in this paper. The equivalent acceleration in this case is defined as

$$a_4 = \beta a_2, \beta > 1, \tag{16}$$

where β is a equivalent coefficient that transfer efficiency into accleration.

To sum up, the payoff matrix is shown in Table II .

C. Decision-Making of Driving Mode

The mixed strategy Nash equilibrium theory is used to solve the optimal strategy, which can solve the probability that the

TABLE III
PARAMETERS OF MPC

Parameter	Value	Parameter	Value
T_s	0.005 s	T_x	0.75 s
N_p	60	N_c	30
$a_{\min}$	-6 m/s^2	$a_{\max}$	3 m/s^2
$v_{\min}$	0 m/s	$v_{\max}$	60 m/s
q	$diag(1,1,1)$	r	0.1

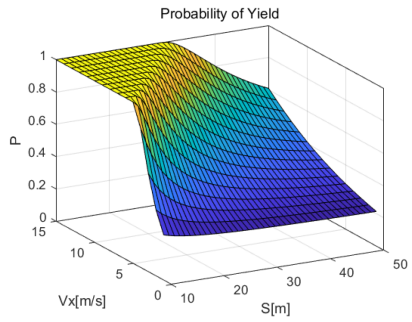

Fig. 8. Probability of "Yield".

player adopts a certain strategy. There are two possible methods to solve mixed strategy Nash equilibrium problem: maximum payoff method and equal payoff method. This paper chooses the equal payoff method to solve mixed strategy Nash equilibrium problem.

Assuming that the probability of the ego vehicle choosing the "yield" strategy is P , so probability of it choosing the "cross" strategy is $1-P$. The principle of equal payoff method is that when the Nash equilibrium is reached, the player's mixed strategy can make own expected payoff equal regardless of any pure strategy adopted by other players, as shown in (17):

$$Pa_2 + (1-P)a_3 = Pa_4 + (1-P)a_1, P \in [0,1]. \quad (17)$$

Solve equation (17),

$$P = \frac{a_3 - a_1}{a_3 + a_4 - a_1 - a_2}. \quad (18)$$

Suppose α is threshold of the driving mode decision. If $P > \alpha$, the ego vehicle selects "yield" mode, otherwise, the ego vehicle selects "cross" mode. The smaller the α is, the more conservative the ego vehicle will behave, and vise versa.

When $D_{safe} = 5$, $\Delta t = 2$,$\beta = 5$, the result of formula (18) to solve the probability that the ego vehicle selects "Yield", is shown in the Fig. 8. It can be seen from Fig. 8 that the probability of the ego vehicle choosing "Yield" is positively correlated with the vehicle speed and negatively correlated with the distance from the conflict point.

IV. MPC-Based Motion Planning

A. Motion Planning

The motion planning in this paper is based on S-T diagram. Different driving modes have different motion planning strategies. If there exist a conflict point between the ego vehicle and the target vehicle, the S-T diagram of the ego vehicle is shown in Fig. 9.

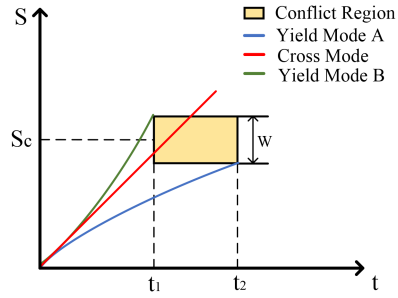

Fig. 9. S-T diagram.

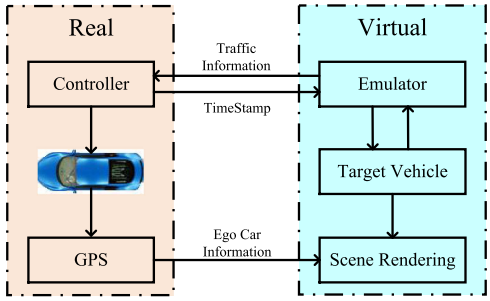

Fig. 10. Test Platform.

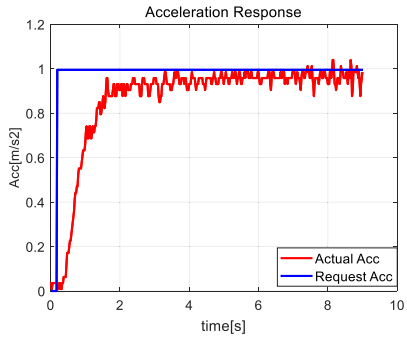

Fig. 11. Acceleration Response.

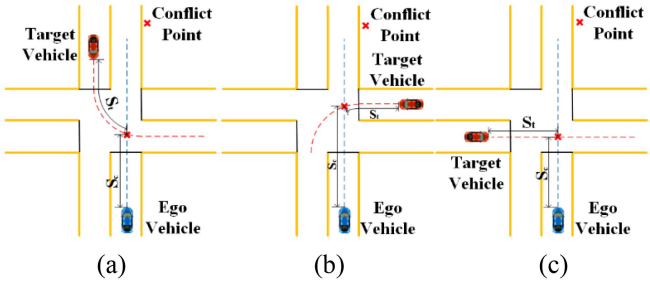

Fig. 12. Test Scenario.

In Fig. 9, t_1 is the time for the head of the target vehicle reaches the conflict point. t_2 is the time for the tail of the target vehicle reaches the conflict point. The yellow region indicates the conflict region, which means that target vehicles will occupy the space of $S_c - \frac{W}{2} \sim S_c + \frac{W}{2}$ during $t_1 \sim t_2$.Windicates the

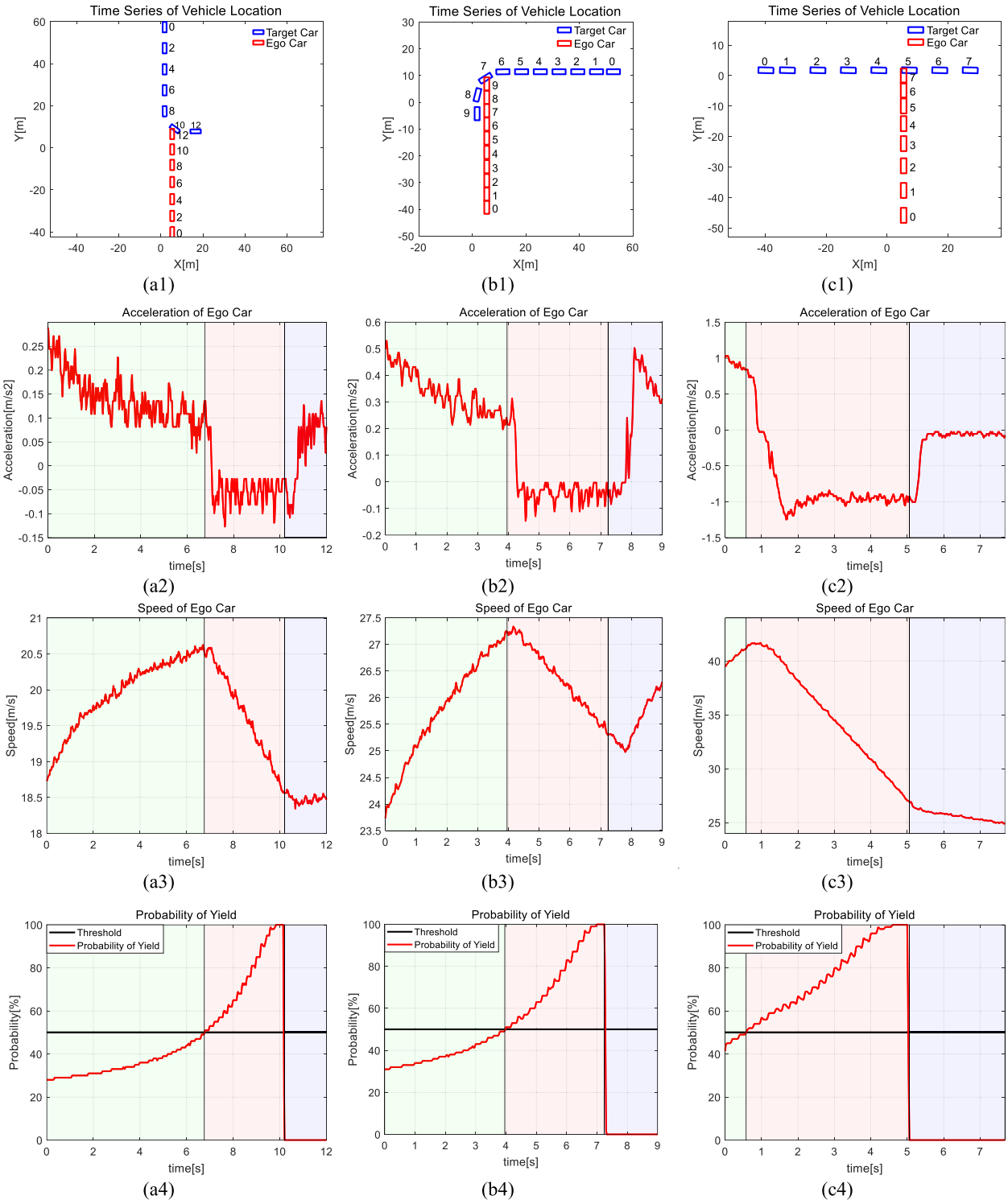

Fig. 13. Test results.

width of the conflict region. If the S-T curve of the ego vehicle passes through the conflict region, it will collide with the target vehicle. If the ego vehicle maintains the initial speed, the S-T curve of the ego vehicle is the red curve in Fig. 9, and the ego vehicle will collide with the target vehicle at time t_1.

According to Newton's second law of motion, the driving distance S and driving time t of the main vehicle meet the formula (19):

$$S(t) = v_0 t + \frac{1}{2} a t^2, \tag{19}$$

where v_0 is the initial speed of the vehicle. a is the acceleration.

In "Cross" mode, the S-T curve of the ego vehicle is a red curve, which means that the main vehicle maintains initial speed. In "Yield" mode, the S-T curve of the ego vehicle is blue curve

("Yield Mode A") or cyan curve ("Yield Mode B"). The blue curve means that the ego vehicle slows down to yield, allowing target vehicle to pass through the conflict region first. Cyan curve is a "generalized" yield, which avoids collision by acceleration.

The acceleration calculation of the two "Yield" modes is shown in (20):

$$\begin{cases} a_{Ap} = \frac{2\left(S_c - \frac{W}{2} - D_{safe} - v_0 t_2\right)}{t_2^2} \\ a_{Bp} = \frac{2\left(S_c + \frac{W}{2} + D_{safe} - v_0 t_1\right)}{t_1^2} \end{cases}. \tag{20}$$

If $-a_{Ap} > a_{Bp}$, $a_p = a_{Bp}$, otherwise, $a_p = a_{Ap}$.

The planned driving distance and speed of the ego vehicle are

$$\begin{cases} S_p(t) = v_0 t + \frac{1}{2} a_p t^2 \\ v_p(t) = v_0 + a_p t \end{cases}. \tag{21}$$

B. MPC Controller for Motion Planning

The longitudinal control algorithm used in this paper is MPC. the longitudinal control model of the vehicle is

$$\underbrace{\begin{bmatrix} S(k+1) \\ v(k+1) \\ a(k+1) \end{bmatrix}}_{\mathbf{x(k+1)}} = \underbrace{\begin{bmatrix} 1 & T_s & 0 \\ 0 & 1 & T_s \\ 0 & 0 & 1-\mathrm{T_s}/T_x \end{bmatrix}}_{\mathbf{A}} \cdot \underbrace{\begin{bmatrix} S(k) \\ v(k) \\ a(k) \end{bmatrix}}_{\mathbf{x(k)}} + \underbrace{\begin{bmatrix} 0 \\ 0 \\ T_s/T_x \end{bmatrix}}_{\mathbf{B}} \underbrace{a_{req}(k)}_{\mathbf{u(k)}}, \tag{22}$$

where $S(k), v(k)$ and $a(k)$ is the travel distance, speed and acceleration of the vehicle at the k-th sampling time respectively. T_s is the sampling time of the controller. T_x is the time constant of the first-order inertial element.$a_{req}(k)$is the requested acceleration of the controller at time k.

The predictive states of the controller are, (23) shown at the bottom of this page, where N_p is the prediction horizon length.$N_c$is the control horizon length.

The cost function for MPC controller is

$$J = (\mathbf{X} - \mathbf{X_r})^T \mathbf{Q} (\mathbf{X} - \mathbf{X_r}) + \mathbf{U}^T \mathbf{R} \mathbf{U}, \tag{24}$$

where the first term is linked to the objective of minimizing the errors between the predicted output and the reference state while the second term reflects the consideration given to the size of $\mathbf{U}$when the cost function J is made to be as small as possible. $\mathbf{X_r}$is reference state from (21).$\mathbf{Q}$is a diagonal matrix in the form that $\mathbf{Q} = \mathbf{q} \cdot \mathbf{I}_{N_p \times N_p}$.$\mathbf{R}$is a diagonal matrix in the form that $\mathbf{R} = \mathbf{r} \cdot \mathbf{I}_{N_c \times N_c}$.$\mathbf{q}$ and $\mathbf{r}$is used as tuning parameters for state variables and input variables.

The system needs to meet the constraints of safety, vehicle dynamics and actuator characteristics. The constraints for $S(k)$, $v(k)$,$a(k)$and $a_{req}(k)$ are defined as follows:

$$\begin{cases} S(k) \notin P \\ v_{\min} \le v(k) \le v_{\max} \\ a_{\min} \le a(k), a_{req}(k) \le a_{\max} \end{cases}, \tag{25}$$

where P is conflict region. $v_{\max}$ is determined by the vehicle dynamics. Because of can't reverse at the intersection, $v_{\min} = 0$. $a_{\min}$ and $a_{\max}$ is determined by the ESP of vehicle.

To find the optimal input variable sequence $\mathbf{U}^* = \arg\min_{\mathbf{U}} J(\mathbf{U})$ that will minimize J, by using (23), J is expressed as

$$\begin{aligned} J &= (\mathbf{X} - \mathbf{X_r})^T \mathbf{Q} (\mathbf{X} - \mathbf{X_r}) + \mathbf{U}^T \mathbf{R} \mathbf{U} \\ &= \mathbf{X}^T \mathbf{Q} \mathbf{X} - \mathbf{X_r}^T \mathbf{Q} \mathbf{X} - \mathbf{X}^T \mathbf{Q} \mathbf{X_r} + \mathbf{X_r}^T \mathbf{Q} \mathbf{X_r} + \mathbf{U}^T \mathbf{R} \mathbf{U} \\ &= (\mathbf{S_x x} + \mathbf{S_u U})^T \mathbf{Q} (\mathbf{S_x x} + \mathbf{S_u U}) - \mathbf{X_r}^T \mathbf{Q} (\mathbf{S_x x} + \mathbf{S_u U}) \\ &\quad - (\mathbf{S_x x} + \mathbf{S_u U})^T \mathbf{Q} \mathbf{X_r} + \mathbf{X_r}^T \mathbf{Q} \mathbf{X_r} + \mathbf{U}^T \mathbf{R} \mathbf{U} \\ &= \mathbf{x}^T \mathbf{S_x}^T \mathbf{Q} \mathbf{S_x x} + \mathbf{U}^T \mathbf{S_u}^T \mathbf{Q} \mathbf{S_x x} + \mathbf{x}^T \mathbf{S_x}^T \mathbf{Q} \mathbf{S_u U} \\ &\quad + \mathbf{U}^T \mathbf{S_u}^T \mathbf{Q} \mathbf{S_u U} - \mathbf{X_r}^T \mathbf{Q} \mathbf{S_x x} - \mathbf{X_r}^T \mathbf{Q} \mathbf{S_u U} - \mathbf{x}^T \mathbf{S_x}^T \mathbf{Q} \mathbf{X_r} \\ &\quad - \mathbf{U}^T \mathbf{S_u}^T \mathbf{Q} \mathbf{X_r} + \mathbf{X_r}^T \mathbf{Q} \mathbf{X_r} + \mathbf{U}^T \mathbf{R} \mathbf{U}, \end{aligned} \tag{26}$$

Ignoring constant terms, the cost function can be expressed as

$$\tilde{J} = \mathbf{U}^T \left(\mathbf{S_u}^T \mathbf{Q} \mathbf{S_u} + \mathbf{R}\right) \mathbf{U} + 2 \left(\mathbf{x}^T \mathbf{S_x}^T \mathbf{Q} \mathbf{S_u} - \mathbf{X_r}^T \mathbf{Q} \mathbf{S_u}\right) \mathbf{U}, \tag{27}$$

It can be seen from (27) that the problem of solving MPC is a quadratic programming problem with constraints:

$$\begin{aligned} &\tilde{J}(\mathbf{U_\Delta}) = \tfrac{1}{2} \mathbf{U_\Delta}^T \mathbf{H} \mathbf{U_\Delta} + \mathbf{F} \mathbf{U_\Delta} \\ &\text{s.t.} \begin{cases} S(k) \notin P \\ v_{\min} \le v(k) \le v_{\max} \\ a_{\min} \le a(k), a_{req}(k) \le a_{\max} \end{cases} \end{aligned} \tag{28}$$

where $\mathbf{H} = 2(\mathbf{S_u}^T \mathbf{Q} \mathbf{S_u} + \mathbf{R})$, $\mathbf{F} = 2(\mathbf{x}^T \mathbf{S_x}^T \mathbf{Q} \mathbf{S_u} - \mathbf{X_r}^T \mathbf{Q} \mathbf{S_u})$.

The interior point method is used to find the optimal control sequence $\mathbf{U}^*$. In this paper, the parameters of MPC are designed as Table III.

$$\underbrace{\begin{bmatrix} \mathbf{x}(k+1) \\ \mathbf{x}(k+2) \\ \vdots \\ \mathbf{x}(k+N_c) \\ \vdots \\ \mathbf{x}(k+N_p) \end{bmatrix}}_{\mathbf{X}} = \underbrace{\begin{bmatrix} \mathbf{A} \\ \mathbf{A}^2 \\ \vdots \\ \mathbf{A}^{N_c} \\ \vdots \\ \mathbf{A}^{N_p} \end{bmatrix}}_{\mathbf{S_x}} \cdot \mathbf{x}(k) + \underbrace{\begin{bmatrix} \mathbf{B} & \mathbf{0} & \mathbf{0} & \mathbf{0} \\ \mathbf{AB} & \mathbf{B} & \mathbf{0} & \mathbf{0} \\ \cdots & \cdots & \ddots & \cdots \\ \mathbf{A}^{N_c-1}\mathbf{B} & \mathbf{A}^{N_c-2}\mathbf{B} & \cdots & \mathbf{B} \\ \cdots & \cdots & \ddots & \cdots \\ \mathbf{A}^{N_p-1}\mathbf{B} & \mathbf{A}^{N_p-2}\mathbf{B} & \cdots & \mathbf{A}^{N_p-N_c-1}\mathbf{B} \end{bmatrix}}_{\mathbf{S_u}} \cdot \underbrace{\begin{bmatrix} a_{req}(k) \\ a_{req}(k+1) \\ \vdots \\ a_{req}(k+N_c-1) \end{bmatrix}}_{\mathbf{U}}, \tag{23}$$

V. Vehicle Test

In order to verify the effectiveness of the framework proposed in this paper, a vehicle test is designed and performed.

A. Test Platform

Safety, efficiency and fidelity have always been a problem perplex researchers in autonomous driving test, since if performed in real world, there will be high risks and low efficiency. Alternatively, if the autonomous driving experiment is performed in the virtual world, it can ensure absolute safety and greatly improve the experimental efficiency, but sacrifice its fidelity of result. In order to balance the fidelity and safety of the test, this paper adopts the combination of real and virtual to performed the autonomous driving test, in which the ego vehicle is real and the target vehicle is virtual, as shown in Fig. 10.

First, the controller sends the timestamp information to the Emulator. The emulator updates the simulation time according to the timestamp information and updates the motion information of the target vehicle. The controller receives the motion information of the target vehicle provided by the emulator as the "perception information" of the ego vehicle. The controller takes the state of the target vehicle and the input of other sensors as " perception information" to control the ego vehicle. The scene rendering system renders the scene according to the ego vehicle information provided by "GPS/IMU" and the target vehicle information calculated by the emulator, so as to achieve the purpose of visualization.

The ego vehicle used in this paper is a modified EU7 from BAIC Motor. The acceleration response of ego vehicle can be regarded as a first-order inertia element $\frac{1}{T_x s+1}$.The acceleration response of the ego vehicle is shown in the Fig. 11.

According to the identification method of the first-order inertial element, the time constant is equal to the time for the output of system rises to 63.2% of the final value. The time constant T_x of the ego vehicle used in this paper is 0.75 seconds.

B. Test Scenario and Results

The vehicle test is performed on a dry and flat field. The test scenario is a two-way two-lane intersection. Three intersection conflict scenarios are tested, as shown in Fig. 12.

The ego vehicle and target vehicle approach the intersection at the speed of 18, 25 and 35 km/h respectively in test scenario (a), (b) and (c). If the ego vehicle and the target vehicle do not change their motion state, they will collide at the conflict point shown in Fig. 12. The algorithm designed in this paper is deployed in the ego vehicle, and the target vehicle keeps the initial speed.

Fig. 13(a1)–(a4), (b1)–(b4) and (c1)–(c4) are the test results of scenario (a), (b) and (c) respectively. The positions of ego vehicle and target vehicle at different times are shown in Fig. 13(a1), (b1) and (c1). In Fig. 13(a4), at $t = 6.8s$, the probability of selecting "Yield" mode calculated by the mixed strategy Nash equilibrium theory is greater than the threshold value of 0.5. At $t = 10s$, the target vehicle passes through the conflict point before the ego vehicle, and the ego vehicle completes the "Yield" process. The light green areas in Fig. 13(a2), (a3) and (a4) are the normal driving stage. At this stage, due to the small "Yield" probability, the ego vehicle does not decide to yield. The light red area is the "Yield" stage. At this stage, because the "Yield" probability exceeds the threshold, the ego vehicle decides to yield and decelerate. The light blue area is the conflict disappearance stage. At this stage, there is no conflict between the ego vehicle and the target vehicle because the target vehicle has left the conflict point/crossroad. It can be seen from Fig. 13(a2), (b2) and (c2) that in the "Yield" mode, the deceleration of the ego vehicle is very small, which can meet the requirements for comfort. In the three scenarios, the decision-making framework proposed in this paper can safely and comfortably avoid collision.

VI. Conclusion

This paper introduces a new decision-making framework in uncontrolled intersection based on intention prediction method and mixed strategy Nash equilibrium theory. The framework is a three-stage method: target vehicle motion prediction, driving mode decision and motion planning. The intention prediction module predicts the driving intention of target vehicles in intersection through the fusion algorithm of GMM-HMM and SVM. The test results show that the prediction result of the fusion algorithm is obviously better than the single algorithm, and the accuracy of intention prediction increases as the target vehicles approach the intersection. If there are conflict points between the trajectory of the target vehicle and the ego vehicle, the mixed strategy Nash equilibrium theory would use to decide whether to avoid the target vehicle. The real vehicle test results show that this method can not only avoid premature or unnecessary deceleration due to conservation, but also avoid collision or violent deceleration due to greed. The motion planning module adopts model predictive control algorithm. The vehicle performance shows that the deceleration calculated by the motion planning module can meet the requirements of safety and comfort. As the proposed decision-making framework fully considers the impact of surrounding vehicles, it can improve the safety and efficiency of the autonomous vehicle in uncontrolled intersections. More precisely, the intention prediction method combining GMM-HMM and SVM improves the accuracy of prediction, which provides valuable information for subsequent decisions and planning. Moreover, by analyzing the interaction process between the surrounding vehicles and the autonomous vehicle, the driving mode decision method based on the mixed strategy Nash equilibrium theory provides a safe and efficient solution to the conflicts. Granted, the decision-making framework only focuses on the regular intersection scenarios, which does not consider the irregular intersection scenarios (three-fork intersection, roundabout and non-orthogonal intersection, etc.). In the future, intersection structure information will be added into the intention prediction module, so that the decision-making framework can handle more intersection scenarios.

References

[1] S. Noh, "Decision-making framework for autonomous driving at road intersections: Safeguarding against collision, overly conservative behavior, and violation vehicles," *IEEE Trans. Ind. Electron.*, vol. 66, no. 4, pp. 3275–3286, Apr. 2019.

[2] M. C. Simon, T. Hermitte, and Y. Page, "Intersection road accident causation: A European view," in *Proc. 21st Int. Tech. Conf. Enhanced Saf. Veh.*, 2009, pp. 1–10.
[3] M. S. Shirazi and B. T. Morris, "Looking at intersections: A survey of intersection monitoring, behavior and safety analysis of recent studies," *IEEE Trans. Intell. Transp. Syst.*, vol. 18, no. 1, pp. 4–24, Jan. 2017, doi: 10.1109/TITS.2016.2568920.
[4] J. Werneke and M. Vollrath, "How do environmental characteristics at intersections change in their relevance for drivers before entering an intersection: Analysis of drivers' gaze and driving behavior in a driving simulator study[J]," *Cognition, Tech. Work*, vol. 16, no. 2, pp. 157–169, 2014.
[5] E.-H. Choi, "Crash factors in intersection-related crashes: An on-scene perspective," WA, DC, USA: Nat. Center Statist. Anal., Nat. Highway Traffific Saf. Admin., Tech. Rep. HS-811 366, 2010.
[6] Crash factors in intersection-related crashes: an on-scene perspective, 2010. [Online]. Available: https://crashstats.nhtsa.dot.gov/Api/Public/ViewPublication/811366
[7] W. Zhan, C. Liu, C. - Y. Chan, and M. Tomizuka, "A non-conservatively defensive strategy for urban autonomous driving," in *Proc. IEEE 19th Int. Conf. Intell. Transp. Syst.*, 2016, pp. 459–464.
[8] Google self-driving car project monthly report, Sep. 2016. [Online]. Available: https://static.googleusercontent.com/media/www.google.com/en//selfdrivingcar/fifiles/reports/report-0916.pdf
[9] R. Rajamani, *Vehicle Dynamics and Control*. New York, NY, USA: Springer, 2006.
[10] M. Brannstrom, E. Coelingh, and J. Sjoberg, "Model-Based threat assessment for avoiding arbitrary vehicle collisions," *IEEE Trans. Intell. Transp. Syst.*, vol. 11, no. 3, pp. 658–669, Sep. 2010.
[11] Z. Ruifeng et al., "A method for connected vehicle trajectory prediction and collision warning algorithm based on V2V communication," *Int. J. Crashworthiness*, vol. 22, no. 1, pp. 15–25, 2017.
[12] B. D. Kim, C. M. Kang, S. H. Lee, C. C. Chung, and J. W. Choi, "Probabilistic vehicle trajectory prediction over occupancy grid map via recurrent neural network," in *Proc. IEEE 20th Int. Conf. Intell. Transp. Syst.*, 2017, pp. 399–404.
[13] L. Lin, W. Li, H. Bi, and L. Qin, "Vehicle trajectory prediction using LSTMs with spatial-temporal attention mechanisms," *IEEE Intell. Transp. Syst. Mag.*, vol. 14, no. 2, pp. 197–208, Mar./Apr. 2022.
[14] Y. Jeong and K. Yi, "Target vehicle motion prediction-based motion planning framework for autonomous driving in uncontrolled intersections," *IEEE Trans. Intell. Transp. Syst.*, vol. 22, no. 1, pp. 168–177, Jan. 2021.
[15] B. Tang, S. Khokhar, and R. Gupta, "Turn prediction at generalized intersections," in *Proc. IEEE Intell. Veh. Symp.*, 2015, pp. 1399–1404.
[16] T. Zhang, W. Song, M. Fu, Y. Yang, and M. Wang, "Vehicle motion prediction at intersections based on the turning intention and prior trajectories model," *IEEE/CAA J. Automatica Sinica*, vol. 8, no. 10, pp. 1657–1666, Oct. 2021.
[17] A. Aksjonov and V. Kyrki, "Rule-based decision-making system for autonomous vehicles at intersections with mixed traffic environment," in *Proc. IEEE Int. Intell. Transp. Syst. Conf.*, 2021, pp. 660–666.
[18] G. Li et al., "Continuous decision-making for autonomous driving at intersections using deep deterministic policy gradient," in *Proc. IET Intell. Transport Syst.*, 2021, pp. 1–13.
[19] S. Zhang, Y. Zhi, R. He, and J. Li, "Research on traffic vehicle behavior prediction method based on game theory and HMM," *IEEE Access*, vol. 8, pp. 30210–30222, 2020.
[20] C. Yang, J. Wang, and J. Dong, "Capacity model of exclusive right-turn lane at signalized intersection considering pedestrian-vehicle interaction," *J. Adv. Transp.*, vol. 2020, no. 5, pp. 1–19, 2020.
[21] M. Elhenawy, A. A. Elbery, A. A. Hassan, and H. A. Rakha, "An intersection game-theory-based traffic control algorithm in a connected vehicle environment," in *Proc. IEEE 18th Int. Conf. Intell. Transp. Syst.*, 2015, pp. 343–347.
[22] C. Cheng, Z. Yang, and D. Yao, "A speed guide model for collision avoidance in non-signalized intersections based on reduplicate game theory," in *Proc. IEEE Intell. Veh. Symp.*, 2018, pp. 1614–1619.
[23] Y. Rahmati, M. K. Hosseini, and A. Talebpour, "Helping automated vehicles with left-turn maneuvers: A game theory-based decision framework for conflicting maneuvers at intersections," *IEEE Trans. Intell. Transp. Syst.*, to be published, doi: 10.1109/TITS.2021.3108409.
[24] C. Hubmann, M. Becker, D. Althoff, D. Lenz, and C. Stiller, "Decision making for autonomous driving considering interaction and uncertain prediction of surrounding vehicles," in *Proc. Intell. Veh. Symp.*, 2017, pp. 1671–1678.
[25] H. Bai, D. Hsu, and W. S. Lee, "Integrated perception and planning in the continuous space: A POMDP approach," *Int. J. Robot. Res.*, vol. 33, no. 9, pp. 1288–1302, 2013.
[26] S. Ulbrich and M. Maurer, "Probabilistic online POMDP decision making for lane changes in fully automated driving," in *Proc. IEEE Int. Conf. Intell. Transp. Syst.*, 2013, pp. 2063–2067.
[27] D. Isele, R. Rahimi, A. Cosgun, K. Subramanian, and K. Fujimura, "Navigating occluded intersections with autonomous vehicles using deep reinforcement learning," in *Proc. IEEE Int. Conf. Robot. Automat.*, 2018, pp. 2034–2039.
[28] G. Schildbach, M. Soppert, and F. Borrelli, "A collision avoidance system at intersections using robust model predictive control," in *Proc. IEEE Intell. Veh. Symp.*, 2016, pp. 233–238.
[29] J. Müller, J. Strohbeck, M. Herrmann, and M. Buchholz, "Motion planning for connected automated vehicles at occluded intersections with infrastructure sensors," *IEEE Trans. Intell. Transp. Syst.*, to be published, doi: 10.1109/TITS.2022.3152628.
[30] A. Pentland and A. Liu, "Modeling and prediction of human behavior," *Neural Comput.*, vol. 11, no. 1, pp. 229–242, 1999, .
[31] C. Cortes, "Support-Vector networks," *Mach. Learn.*, vol. 20, pp. 273–297, 1995.
[32] G. Casella and R. L. Berger, "Statistical inference," *Technometrics*, vol. 33, 1990, Art. no. 4.
[33] L. E. Baum, "An inequality and associated maximization technique in statistical estimation for probablistic functions of Markov processes," in *Proc. 3rd Symp. Inequalities*, 1972, pp. 1–8.
[34] J. C. Platt, "Fast training of support vector machines using sequential minimal optimization, advances in kernel methods," in *Advances in Kernel Methods: Support Vector Learning*. Cambridge, MA, USA: MIT Press, 1999.

Jiangfeng Nan received the B.S. degree from North China Electric Power University, Beijing, China, in 2017, and the M.S. degree from the Beijing Institute of Technology, Beijing, China, in 2019. He is currently working toward the Ph.D. degree in vehicle engineering with Beihang University, Beijing, China. His research interests include intelligent driving strategy, dynamics and controls, and autonomous driving.

Weiwen Deng (Member, IEEE) received the B.S. degree in aeronautical manufacturing from Nanjing Aeronautical Institute, Nanjing, China, in 1983, and the M.S. degree in mechanical design from Beihang University, Beijing, China, in 1989, and the Ph.D. degree in electrical and computer engineering from Oakland University, Oakland, CA, USA, in 2004. He is currently a Distinguished Professor and the Dean of the School of Transportation Science and Engineering, Beihang University. Prior to that, he was Researcher with General Motors R&D Center, USA. He holds more than 70 patents, and is the authoror coauthor of more than 140 peer-reviewed international journal and conference papers. His primary research interests include dynamics and controls, modeling and simulation on intelligent, and electric vehicles.

Bowen Zheng received the B.Sc. degree in electrical engineering from Ohio State University Columbus, OH, USA, and the M.Sc. degree in technological systems management from SUNY-Stony Brook University, Stony Brook, NY, USA. He is currently working toward the Ph.D. degree in vehicle engineering with Beihang University, Beijing, China. Prior to that, he was a Electrical Architecture Engineer and Diagnostic Development Engineer with BAIC Motor Inc. for more than two years. He holds two patents with another one pending. His research interests include wire-controlled chassis system, hardware and software architecture, and functional safety.